Comparison of adaptive algorithms for the control of tonal disturbances in mechanical systems

M Zilletti, S J Elliott and J Cheer

Institute of Sound and Vibration Research, University of Southampton, University Road, Southampton, SO17 1BJ, UK

E-mail: m.zilletti@soton.ac.uk

Abstract. This paper presents a study on the performance of adaptive control algorithms designed to reduce the vibration of mechanical systems excited by a harmonic disturbance. The mechanical system consists of a mass suspended on a spring and a damper. The system is equipped with a force actuator in parallel with the suspension. The control signal driving the actuator is generated by adjusting the amplitude and phase of a sinusoidal reference signal at the same frequency as the excitation. An adaptive feedforward control algorithm is used to adapt the amplitude and phase of the control signal, to minimise the mean square velocity of the mass. Two adaptation strategies are considered in which the control signal is either updated after each period of the oscillation or at every time sample. The first strategy is traditionally used in vibration control in helicopters for example; the second strategy is normally referred to as the filtered-x least mean square algorithm and is often used to control engine noise in cars. The two adaptation strategies are compared through a parametric study, which investigates the influence of the properties of both the mechanical system and the control system on the convergence speed of the two algorithms.

1. Introduction

In this paper an adaptive feedforward control system, to reduce of the vibration of a single-degree-of-freedom system excited by a harmonic force is considered.

Adaptive feedforward control methods have a long history in the active control of tonal disturbances. The first application of active feedforward control was proposed by Leug [1]. The control system was implemented with the aim of reducing the propagation of an acoustic wave in a duct. In this first application the controller was fixed, but Conover [2] suggested that the amplitude and phase of the secondary wave could be manually adjusted to minimise the sound pressure level measured by an error microphone placed downstream. Conover also introduced the idea of an electrical reference for tonal disturbances derived from the primary source, which in his case was a transformer, although tachometers have since been widely used to derive such electrical reference signals for primary sources such as engines and rotors. Since then the development of signal processing and control theory, together with the development of low cost digital signal processing boards, has paved the way of more effective implementations. Adaptive filters based on least mean square (LMS) algorithms have been widely used in this application, although the dynamic response between the secondary source and the error sensor may cause instability when the classical LMS algorithm is implemented. Therefore a modified form of the LMS algorithm, called filtered-x least mean square (FxLMS) algorithm, was developed to improve the control performance [3, 4]. The latter

algorithm uses a reference signal filtered through a model of the secondary path, often called plant model in the control literature, which is then used as the reference signal for the standard LMS algorithm. The stability and performance of FxLMS algorithm depend on the accuracy of the plant model [3-5]. The adaptation of the FxLMS algorithm is normally carried out at every sample time in which case an equivalent feedback representation of the algorithm can be derived [6, 7]. In some applications, such as the active vibration control in helicopter cabins [8-11], the adaptation is carried out at every period of the oscillation. As shown in reference [12] a period by period adaptation may be employed in the vibration control of mechanical systems characterised by nonlinear damping. In this case, due to the nonlinear damping, the response of the system depends on the excitation level, thus the plant model needs to be updated at every period of the oscillation in order to improve the convergence time. The sample by sample and the period by period adaptations are both well-established algorithms for harmonic control [6] and [13]. The work presented in this paper aims to compare the convergence properties of these two types of adaptation. This is important in the design of practical algorithms for harmonic control in order to guarantee the best convergence and performance depending on the properties of the system under control and parameters of the control system.

In this paper the performance of two adaptation strategies in controlling the vibration of a single degree of freedom system excited by a harmonic force are compared. The aim of the study is to investigate the influence of the properties of both the mechanical system and the control system on the convergence speed of the two algorithms. The analysis is based on the assumption that the disturbance is periodic with known fixed frequency. In practical systems, the reference signal can be measured using a sensor (e.g. tachometers, accelerometers, or microphones depending on the application). If the frequency of the disturbance does not vary with time, a synthetic reference signal may also be used. If the frequency of the disturbance is time variant specific control algorithms may be employed[14].

In this paper the equivalent feedback formulations for the two adaptation algorithm are derived in section 2. Simulation results on the vibration control of a single-degree-of-freedom system are presented in section 3 and conclusions are drawn in section 4.

2. Mathematical model

Figure 1 shows the single degree of freedom (SDOF) system considered in this study, consisting of a mass m suspended on a spring of stiffness k in parallel with a damper of mechanical damping c. The physical parameters of the system under control considered in the simulation results are summarised in Table 1.

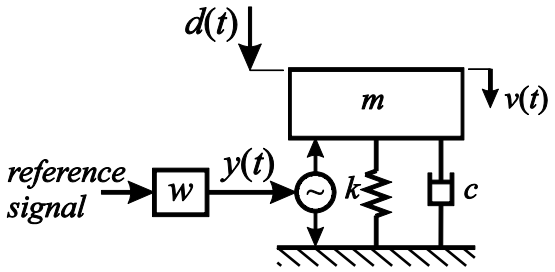

Figure 1. Schematic diagram of a single degree-of-freedom system with the controller.

The system under control is equipped with an ideal force actuator in parallel with the passive suspension. A substantial reduction of the velocity of mass m can be achieved by feeding the actuator with a harmonic control signal y with the same frequency of the disturbance d and an appropriate magnitude and phase. The control signal y can be generated by adapting the amplitude and phase of a reference harmonic signal to minimize the velocity $v(t)$ of mass m, using an iterative gradient descent algorithm, for example.

Table 1. Physical parameters of the single-degree-of-freedom-system.

Parameters	Value
Mass	$m = 1$ kg
Mechanical stiffness	$k = 3940$ N/m
Mechanical linear damping	$c_1 = \text{variable}$
Natural frequency	$\omega_n = 2\pi \times 10$ rad/s
Disturbance amplitude	$D = 1$ N
Disturbance frequency	$\omega = 2\pi \times 9$ rad/s
Disturbance force	$d(t) = D\sin(\omega t + \phi_d)$

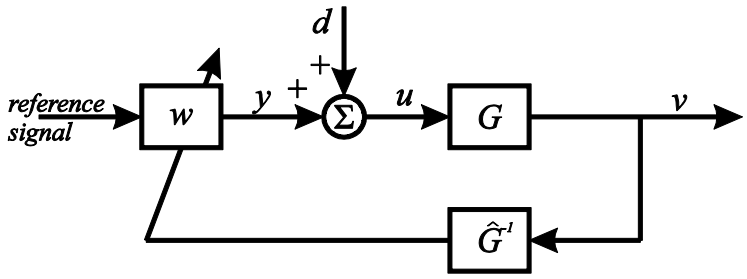

Figure 2: Schematic diagram of the adaptive feedforward control system for the system shown in figure 1. The oblique arrow indicates that the amplitude and phase of the reference signal are adapted in order to minimize the mean square error velocity.

Figure 2 shows a block diagram of an adaptive feedforward control algorithm, where the oblique arrow indicates that the amplitude and phase of the reference signal are updated in order to minimize the mean squared error velocity v. The blocks G and $\hat{G}$ represent the physical plant and the plant model respectively. In this study two adaptation strategies are considered in which the control signal is either updated at every time sample or after each period of the oscillation. For each of the two updating strategies an equivalent feedback formulation is derived in the following two subsections.

2.1. Equivalent feedback formulation for the sample by sample adaptation

The iterative least square algorithm that minimizes the mean square value of the error velocity is given by:

$$\boldsymbol{w}(n+1) = \boldsymbol{w}(n) - \alpha v(n)\boldsymbol{x}_f(n), \tag{1}$$

where $\boldsymbol{w}(n)$ is the vector containing the two coefficients of the controller for the adjustment of the in-phase and quadrature component of the control signal respectively, $v(n)$ is the velocity error signal at the n-th sample time and α is a convergence coefficient. This is an implementation of the FxLMS algorithm for a tonal reference signal. Finally $\boldsymbol{x}_f(n)$ is the vector of the filtered reference signals given by

$$\boldsymbol{x}_f(n) = \begin{bmatrix} r_s(n) \\ r_c(n) \end{bmatrix} = \begin{bmatrix} \mathrm{Re}\{\hat{G}\} & \mathrm{Im}\{\hat{G}\} \\ -\mathrm{Im}\{\hat{G}\} & \mathrm{Re}\{\hat{G}\} \end{bmatrix} \begin{bmatrix} s(n) \\ c(n) \end{bmatrix} \tag{2}$$

where $s(n)$ and $c(n)$ are the instantaneous sine and cosine reference signals respectively and $\hat{G}$ is the complex plant model. Substituting equation (2) in (1) yields:

$$\begin{bmatrix} w_1(n+1) \\ w_2(n+1) \end{bmatrix} = \begin{bmatrix} w_1(n) \\ w_2(n) \end{bmatrix} - \alpha(n)v(n) \begin{bmatrix} r_s(n) \\ r_c(n) \end{bmatrix}. \tag{3}$$

In order to obtain an equivalent feedback formulation for the FxLMS algorithm of equation (3) a complex frequency domain discrete representation will be used. The filtered reference signals $r_s(n)$ and $r_c(n)$ can also be written in exponential form as:

$$r_s(n) = A\sin(\omega_0 n + \phi) = \frac{A}{2j}(e^{j(\omega_0 n+\phi)} - e^{-j(\omega_0 n+\phi)}),$$
$$r_c(n) = A\cos(\omega_0 n + \phi) = \frac{A}{2}(e^{j(\omega_0 n+\phi)} + e^{-j(\omega_0 n+\phi)}) \quad (4)$$

where $A = |\hat{G}|$ is the modulus and $\phi = \angle\hat{G}$ is the phase of the plant model at the excitation frequency ω and $\omega_0 = \omega T$ where T is the sampling period. Using equations (4) the terms $v(n)r_s(n)$ and $v(n)r_c(n)$ can be rewritten as:

$$v(n)r_s(n) = \frac{A}{2}v(n)(-e^{j\omega_0 n}e^{j\phi} + e^{-j\omega_0 n}e^{-j\phi}),$$
$$v(n)r_c(n) = \frac{A}{2}v(n)(e^{j\omega_0 n}e^{j\phi} + e^{-j\omega_0 n}e^{-j\phi}) \quad (5)$$

z-transforming equations (5) yields:

$$Z\{v(n)r_s(n)\} = -\frac{A}{2}e^{j\phi}Z\{e^{j\omega_0 n}v(n)\} + \frac{A}{2}e^{-j\phi}Z\{e^{-j\omega_0 n}v(n)\},$$
$$Z\{v(n)r_c(n)\} = \frac{A}{2}e^{j\phi}Z\{e^{j\omega_0 n}v(n)\} + \frac{A}{2}e^{-j\phi}Z\{e^{-j\omega_0 n}v(n)\}. \quad (6)$$

Recalling that:

$$\mathrm{Z}\{a^n f(n)\} = F\left(\frac{z}{a}\right), \quad (7)$$

where $F(z) = Z\{f(n)\}$ equations (9) can be written(4) as:

$$\mathrm{Z}\{v(n)r_s(n)\} = \frac{A}{2}\left[-je^{j\phi}V\left(ze^{-j\omega_0}\right) + je^{-j\phi}V(ze^{j\omega_0})\right], \quad (8)$$

$$\mathrm{Z}\{v(n)r_c(n)\} = \frac{A}{2}\left[e^{j\phi}V\left(ze^{-j\omega_0}\right) + e^{-j\phi}V(ze^{j\omega_0})\right], \quad (9)$$

where $V(z) = Z\{v(n)\}$. Substituting equations (8) and (9) in (3), the z-transform of $w_1(n)$ and $w_2(n)$ are given by:

$$Z\{w_1(n+1)\} = Z\{w_1(n)\} - \frac{\alpha A}{2}\left[-je^{j\phi}V\left(ze^{-j\omega_0}\right) + je^{-j\phi}V(ze^{j\omega_0})\right], \quad (10)$$

$$Z\{w_2(n+1)\} = Z\{w_2(n)\} - \frac{\alpha}{2}A\left[e^{j\phi}V\left(ze^{-j\omega_0}\right) + e^{-j\phi}V(ze^{j\omega_0})\right], \quad (11)$$

Recalling that $zF(z) = Z\{f(n+1)\}$ equations (10) and (11) can be rewritten as:

$$W_1(z) = -\frac{\alpha A}{2}U(z)\left[-je^{j\phi}V\left(ze^{-j\omega_0}\right) + je^{-j\phi}V(ze^{j\omega_0})\right], \quad (12)$$

$$W_2(z) = -\frac{\alpha}{2}U(z)A\left[e^{j\phi}V\left(ze^{-j\omega_0}\right) + e^{-j\phi}V(ze^{j\omega_0})\right], \quad (13)$$

where $U(z) = 1/(z-1)$. According to the scheme shown in Figure 2, the control signal $y(n)$ is given by

$$y(n) = \boldsymbol{x}^T(n)\boldsymbol{w}(n), \quad (14)$$

where $\boldsymbol{x}$ is the vector of the reference signals given by

$$\boldsymbol{x}(n) = \begin{bmatrix}\sin(\omega_0 n)\\ \cos(\omega_0 n)\end{bmatrix} = \begin{bmatrix}\frac{1}{2j}(e^{j\omega_0 n} - e^{-j\omega_0 n})\\ \frac{1}{2}(e^{j\omega_0 n} + e^{-j\omega_0 n})\end{bmatrix}. \quad (15)$$

Substituting equation (15) in (14) the control signal $y(n)$ can be written as

$$y(n) = \frac{1}{2j}\left(e^{j\omega_0 n} - e^{-j\omega_0 n}\right)w_1(n) + \frac{1}{2}\left(e^{j\omega_0 n} + e^{-j\omega_0 n}\right)w_2(n). \quad (16)$$

Following the same procedure the z-transform of $y(n)$ can be written as

$$Y(z) = \frac{1}{2}\left[-jW_1\left(ze^{-j\omega_0}\right) + jW_1(ze^{j\omega_0})\right] + \frac{1}{2}\left[W_2\left(ze^{-j\omega_0}\right) + W_2(ze^{j\omega_0})\right], \quad (17)$$

and substituting equation (12) and (13) in (17) yields

$$
\begin{aligned}
Y(z) = \frac{1}{2}\Big[& -j\left(-\frac{\alpha A}{2}U\left(ze^{-j\omega_0}\right)\left[-je^{j\phi}V\left(ze^{-2j\omega_0}\right)+je^{-j\phi}V(z)\right]\right) \\
& +j\left(-\frac{\alpha A}{2}U\left(ze^{j\omega_0}\right)\left[-je^{j\phi}V(z)+je^{-j\phi}V\left(ze^{2j\omega_0}\right)\right]\right) \\
& +\left(-\frac{\alpha A}{2}U(ze^{-j\omega_0})\left[e^{j\phi}V\left(ze^{-2j\omega_0}\right)+e^{-j\phi}V(z)\right]\right) \\
& +\left(-\frac{\alpha A}{2}U(ze^{j\omega_0})\left[e^{j\phi}V(z)+e^{-j\phi}V(ze^{2j\omega_0})\right]\right)\Big],
\end{aligned}
\tag{18}
$$

which after some algebraic manipulations leads to

$$
Y(z) = -\frac{\alpha A}{2}\left\{V(z)\left[U\left(ze^{-j\omega_0}\right)e^{-j\phi}+U\left(ze^{j\omega_0}\right)e^{j\phi}\right]\right\}. \tag{19}
$$

Substituting the expression of $U(z) = 1/(z-1)$, equation (19) can be written as:

$$
Y(z) = -\alpha A\left[\frac{z\cos(\omega_0-\phi)-\cos(\phi)}{z^2-2z\cos(\omega_0)+1}\right]V(z) = -\alpha K(z)V(z) \tag{20}
$$

The z-transform of the error is given by

$$
V(z) = [D(z)+Y(z)]G(z) \tag{21}
$$

where $D(z)$ is the z-transform of the disturbance and $G(z)$ is the z-transform of the system transfer function. Substituting equation (20) in (21), $V(z)$ can be written as:

$$
V(z) = \frac{G(z)}{1+\alpha K(z)G(z)}D(z) \tag{22}
$$

As also shown in references [6, 7], Equation (22) represents a closed loop response function of a linear time invariant system which can be represented by the block diagram shown in Figure 5. One advantage of the equivalent feedback formulation is that the stability and performance of the FxLMS algorithm can be assessed by using the classical feedback control theory for time invariant linear system.

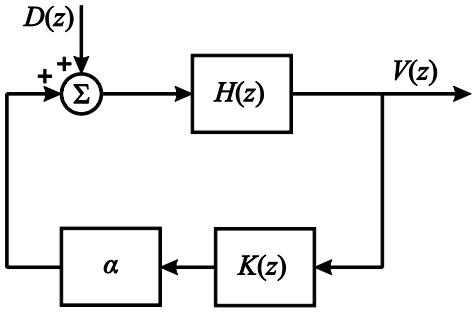

Figure 3: Time domain equivalent feedback for FxLMS algorithm with a tonal reference signal.

2.2. Equivalent feedback formulation for the period by period adaptation

The amplitude and phase of the disturbance d and control signal y with respect to the reference signal can be described by complex numbers, while $\tilde{G}$ denotes the complex response of the physical system under control and $\hat{G}$ represents the complex plant model. The complex control signal $\tilde{y}$ is obtained by multiplying a reference signal, with the same frequency of the disturbance d, by the complex coefficient $\tilde{w}$ where the symbol $\sim$ is used to indicate a complex quantity. Assuming the system response is in the steady state, the iterative least square algorithm that minimizes the cost function $J = \tilde{v}^H\tilde{v}$ is given by:

$$
\tilde{w}(n+1) = \tilde{w}(n) - \alpha\hat{G}^{\dagger}\tilde{v}(n), \tag{23}
$$

where $\tilde{w}(n)$ is the complex response of the controller at the n-th time sample, which has the adjustment of the in-phase component of the control signal as its real part and the quadrature component as its imaginary part, α is an adaptation coefficient and $\hat{G}^{\dagger}$ is, in general, the pseudo-

inverse of the estimated complex plant response at the excitation frequency, which reduces to the scalar inverse in this single channel case. In the single channel case, this iterative least square algorithm can also be considered as a form of normalized gradient descent algorithm

$$\tilde{w}(n+1) = \tilde{w}(n) - \alpha \hat{G}^H \tilde{v}(n), \tag{24}$$

where $\hat{G}^H$ is the complex conjugate of G.

As shown in reference [13], a convenient way to describe the system dynamics is by using an equivalent frequency domain feedback formulation. The analysis is easiest to follow considering first the response of the system to a step change in the coefficient of the controller. This is useful since the output of the controller y is a sinusoidal signal which undergoes changes as the output coefficients are updated. A unit step change, $\tilde{w}(n)$, in the control coefficient at the sample time $n = 0$ produces a time output $y(n)$ given by:

$$y(n) = \mathrm{Re}\{e^{jn\omega}\tilde{w}(n)\}. \tag{25}$$

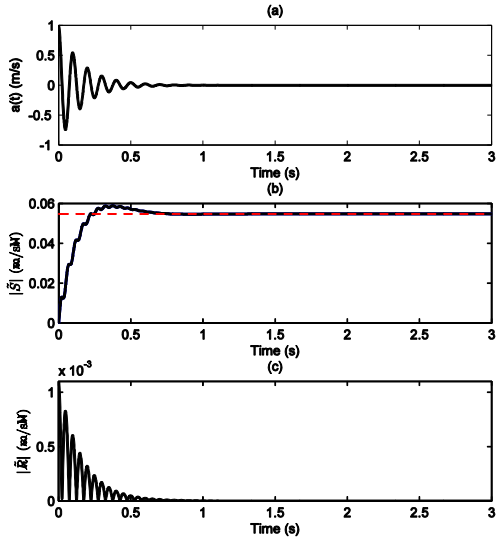

Figure 4: (a) Impulse response $a(t)$, (b) magnitude of the complex step response with $|\tilde{G}|$ shown with the dashed line and (c) the magnitude of complex impulse response.

The time velocity of the mass $v(n)$ is given by:

$$v(n) = \sum_{m=0}^{\infty} a(m)y(n-m), \tag{26}$$

where $a(m)$ is the system time impulse response shown in Figure 4 (a) characterised by the oscillating exponential decay behaviour typical of a linear lightly damped system. Substituting equation (25) in (26) yields:

$$v(n) = \mathrm{Re}\left\{\sum_{m=0}^{\infty} a(m)e^{j(n-m)\omega}\tilde{w}(n-m)\right\} = \mathrm{Re}\left\{e^{jn\omega}\sum_{m=0}^{\infty} a(m)e^{-jm\omega}\tilde{w}(n-m)\right\}, \tag{27}$$

and noticing that $\tilde{w}(n-m)$ is equal one for $m \leq n$ and zero otherwise, equation (27) can be written as:

$$v(n) = \mathrm{Re}\left\{e^{jn\omega}\sum_{m=0}^{n} a(m)e^{-jm\omega}\right\} = \mathrm{Re}\{e^{jn\omega}\tilde{S}(n,\omega)\}, \tag{28}$$

where $\tilde{S}(n,\omega)$ is the complex step response of the system given by:

$$\tilde{S}(n,\omega) = \sum_{m=0}^{n} a(m)e^{-jm\omega}. \tag{29}$$

Figure 4(b) shows the magnitude of the complex step response. Since the impulse response $a(m)$ decays due to the damping in the system after a settling time T_0, $S(n,\omega)$ will tend to a finite value coinciding with the frequency response function of the system $\tilde{G}(\omega)$ shown by the dashed line in Figure 4(b). During the adaptation of the control algorithm, the controller coefficients can be written as the summation of a series of step changes:

$$\widetilde{w}(n) = \sum_{m=-\infty}^{n} \widetilde{w}(m) - \widetilde{w}(m-1) = \sum_{m=-\infty}^{n} \delta_{\widetilde{w}}(m). \tag{30}$$

The complex error velocity $\tilde{v}(n)$ is given by the response due to the disturbance signal $\tilde{d}(n)$ and the contributions from the step changes in controller coefficients thus:

$$\tilde{v}(n) = \tilde{S}(n,\omega)\tilde{d}(n) + \sum_{m=0}^{\infty} \tilde{S}(m,\omega)\delta_{\widetilde{w}}(n-m). \tag{31}$$

Equation (31) can be written as:

$$\tilde{v}(n) = \tilde{d}(n)\sum_{m=0}^{\infty} \tilde{R}(m,\omega) + \sum_{m=0}^{\infty} \tilde{R}(m,\omega)\widetilde{w}(n-m). \tag{32}$$

Where $\tilde{R}(m,\omega)$ is the *frequency domain impulse response* of the system given by:

$$\tilde{R}(m,\omega) = \tilde{S}(m,\omega) - \tilde{S}(m-1,\omega) \quad \text{with} \quad \tilde{S}(-1,\omega) = 0 \tag{33}$$

As shown in Figure 4(c), $\tilde{R}(m,\omega)$ tends to zero when n tends to infinity thus the summations in equation (32) can be carried out only for the first T_0 terms leading to:

$$\tilde{v}(n) = \tilde{d}(n)\sum_{m=0}^{T_0} \tilde{R}(m,\omega) + \sum_{m=0}^{T_0} \tilde{R}(m,\omega)[\widetilde{w}(n-m)]. \tag{34}$$

Z-transforming equation (34) yields:

$$\tilde{V}(z) = \widetilde{H}(z)\big[\widetilde{D}(z) + \widetilde{W}(z)\big]. \tag{35}$$

Where $\tilde{V}(z)$ and $\widetilde{D}(z)$ are the complex z-transforms of $\tilde{v}(n)$ and $\tilde{d}(n)$ and $\widetilde{H}(z)$ is given by:

$$\widetilde{H}(z) = \tilde{R}(0,\omega) + \tilde{R}(1,\omega)z^{-1} + \cdots + \tilde{R}(T_0,\omega)z^{-T_0}. \tag{36}$$

Z-transforming equation (24) yields to:

$$\widetilde{W}(z-1) = \widetilde{W}(z) - \alpha\hat{G}^H\tilde{V}(z), \tag{37}$$

which can be written as:

$$(z-1)\widetilde{W}(z) = -\alpha\hat{G}^H\tilde{V}(z), \tag{38}$$

And thus

$$\widetilde{W}(z) = -\alpha\frac{\hat{G}^H}{z-1}\tilde{V}(z) = -\alpha\tilde{C}(z)\tilde{V}(z), \tag{39}$$

Substituting equation (39) in (35) yields:

$$\tilde{V}(z) = \frac{\widetilde{H}(z)}{1+\alpha\tilde{C}(z)\widetilde{H}(z)}\widetilde{D}(z). \tag{40}$$

As also shows in reference [13], Equation (40) represents a closed loop response function of a linear time invariant system which can be represented by the block diagram shown in Figure 5 (a). The error signal of the linear time invariant feedback loop shown in the Figure 5 (a) is the instantaneous

complex error velocity which cannot be directly measured in a practical system. One way to estimate the complex error at each time sample n is by calculating the FFT of the signal recorded for a period T of the excitation. When the control signal is updated every cycle of the excitation using equation (24) the equivalent feedback scheme can be modified as shown in Figure 5(b) where a sample and hold (S/H) block has been added in the feedback path. The S/H block samples the control signal every cycle of the excitation and holds it for one period. It is important to notice that the feedback loop has different sampling rates: f_s/f_e sample per period for the plant and one sample per period in the feedback path where f_s is the sampling frequency and f_e is the excitation frequency. Therefore in this case the classical control theory for time invariant feedback systems cannot be used to assess the stability of the controller [15].

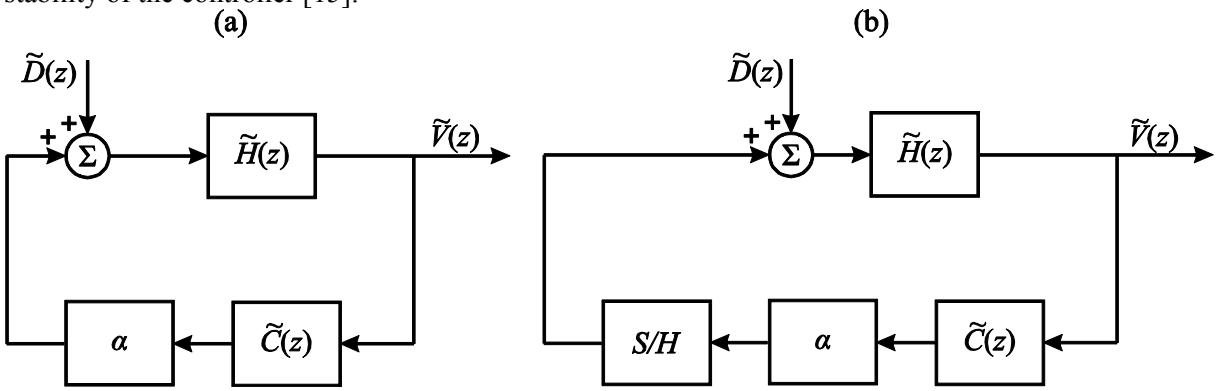

Figure 5: (a) frequency domain equivalent feedback and (b) equivalent feedback of the cycle by cycle update algorithm

3. Simulation results

In this section simulation results on the convergence of the control system are presented when the two adaptation strategies are considered.

The left plots in Figure 6 show the time history of the error when the adaptation of the algorithm is carried out at every sample time for three different value of the convergence coefficient α. The convergence of the algorithm has been simulated in Matlab either by using the feedback formulation presented in section 2.1 (black line) or integrating the equation of motion with the ODE45 (red line). The graphs confirm that the two formulations are equivalent. It can be also noticed that the convergence time improves when α increases. However, for values of α approaching the maximum stable convergence coefficient, α_{max}, the convergence time starts to increase again.

The right plots in Figure 6 (b) show the time history of the velocity when the adaptation of the algorithm is carried out at every period of the oscillation. The simulations are performed in Matlab either using the feedback formulation described in section 2.2 or integrating the equation of motion of the system with the ODE45. In the latter case the complex error signal $\tilde{v}(n)$, at the n-th iteration step is calculated from the time history of the error signal by numerically integrating the equation of motion of the system over one period of the oscillation and calculating the FFT of the signal at the excitation frequency. After the $(n+1)-th$ iteration, $\tilde{w}(n+1)$ is calculated using equation (24) and the time domain simulation is restarted setting as initial condition the state vector at the instant before the $(n+1)-th$ update event. Also in this case the red and black lines show that the two formulations are equivalent. It should be noticed that α_{max} has been calculated for the system without sample and hold described by the block diagram in Figure 5 (a). The effect of the sample and hold block in the feedback path is to destabilize the feedback such that the actual value of the maximum stable gain is lower when the S/H is included in the feedback path.

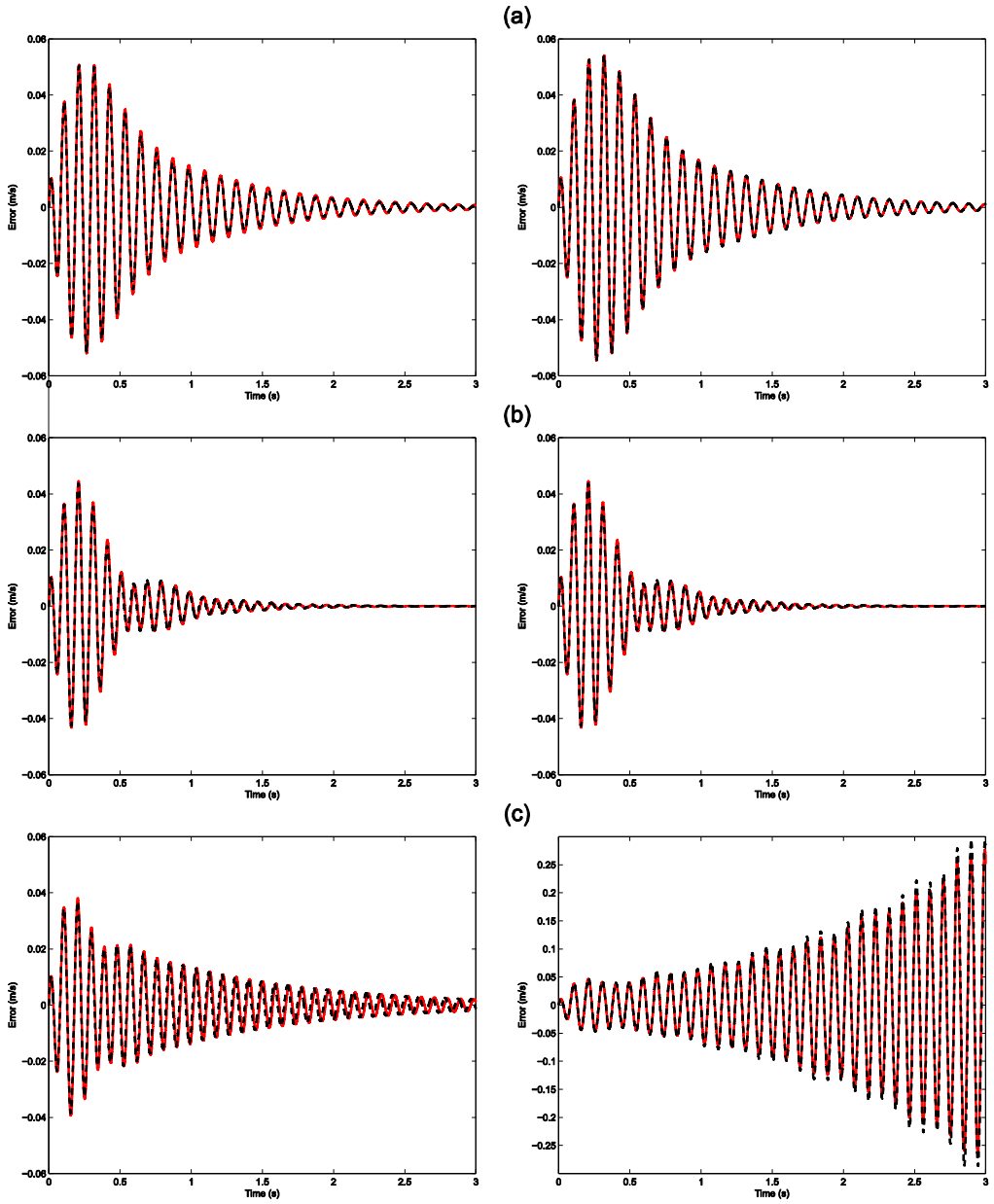

Figure 6: time history of the error velocity when the control signal is either updated at every time sample (left plots) or after each period of the oscillation (right plots) when the convergence coefficient α is set to (a) $\alpha_{max}/10$, (b) $\alpha_{max}/3$ and $\alpha_{max}/1.5$. The simulations are carried out in Matlab directly integrating the equation of motion with the ODE45 (black line) or by using the equivalent feedback formulation (red line).

3.1. Parametric study

In this subsection the effects of the number of sample per period and the damping ratio of the system under control on the convergence time of the control system are investigated. Figure 7 shows the optimal value of the convergence coefficient α that minimise the convergence time when the damping ratio of the system under control is either $\zeta = 0.1$ (a) or $\zeta = 0.5$ (b).

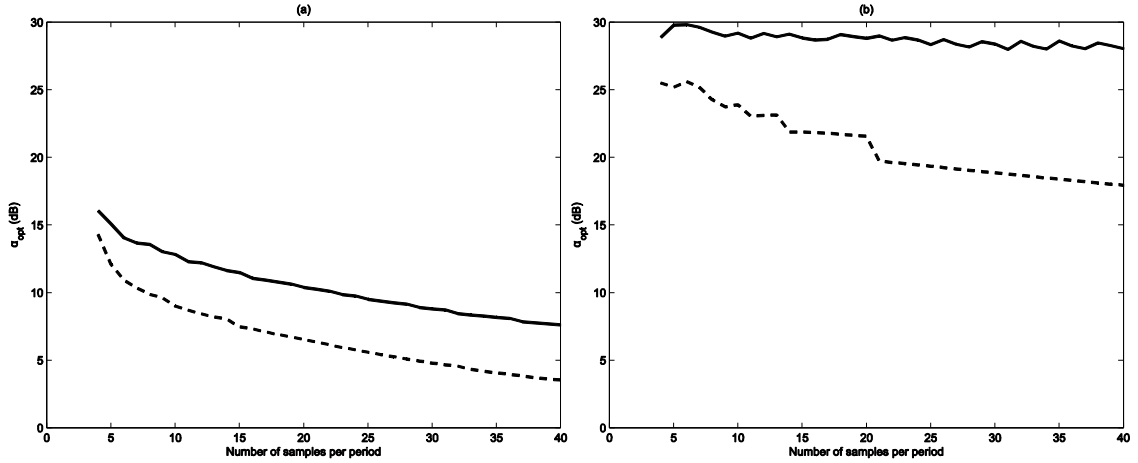

Figure 7: optimal convergence coefficient α as a function of the number of sample per period when the damping ratio is either $\zeta = 0.1$ (a) or $\zeta = 0.5$ (b). Sample by sample adaptation (solid line) and period by period adaptation (dashed line).

The solid and dashed lines in Figure 7 shows the optimal convergence coefficient when the adaptation is carried out at every sample time or at every period of the oscillation respectively. The convergence time τ_c is defined as:

$$\tau_c = n_c f_s \quad \Rightarrow \quad \bar{v}^2(n_c) = \frac{\bar{v}_0^2}{10^3}, \tag{41}$$

where $\bar{v}^2$ and $\bar{v}_0^2$ are the mean square values of the steady state error velocity with and without control respectively and f_s is the sampling frequency. In order to avoid sudden jumps in the curves due to rapid variation of the error signal occurring mainly when high values of α are implemented, the mean square value of the signals have been smoothed using a moving average filter with a length of 5 periods. Figure 7 shows that in general the optimal value of α decreases with the number of samples per period. When the damping ratio of the system under control increases (plot (b)), thus its time constant gets smaller the adaptation can be carried out more rapidly and thus the optimal value of α increases.

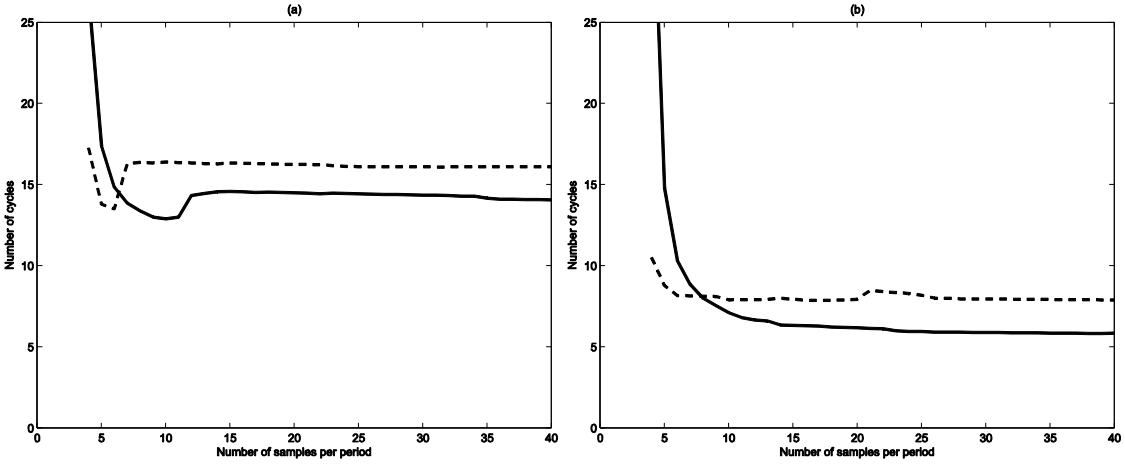

Figure 8: optimal convergence time measured in number of cycle α as a function of the number of sample per period when the damping ratio is either $\zeta = 0.1$ (a) or $\zeta = 0.5$ (b). Sample by sample adaptation (solid line) and period by period adaptation (dashed line).

Figure 8 shows the convergence time when the damping ratio is either $\zeta = 0.1$ (a) or $\zeta = 0.5$ (b) as a function of the number of samples per period. The graphs show that at low sampling rate the convergence of the algorithm when the control signal is updated at every sample (solid line) is slower than the adaptation carried out at every period (dashed line).

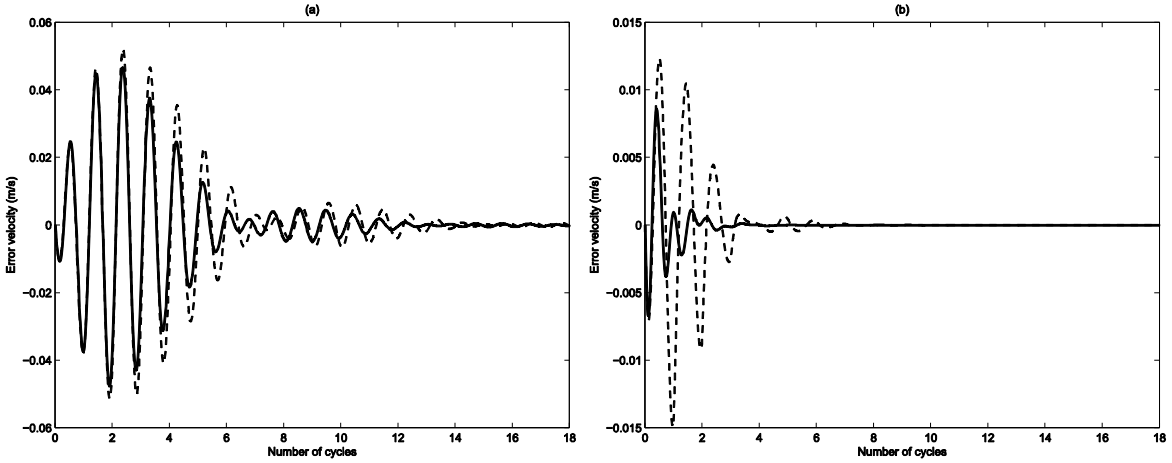

Figure 9: error velocity using the sample by sample adaptation (solid line) or the period by period adaptation (dashed line) algorithms when (a) $\zeta = 0.1$ or (b) $\zeta = 0.5$. The error signal is sampled 40 times per period and the convergence coefficient α is set to the optimal value that minimise the convergence time.

However for higher sampling rate the convergence gets faster if the adaptation is carried out at every sample. Comparing plot (a) and (b) it can be noticed that the convergence time decreases when the damping ratio of the system under control increases. To better understand the difference between the two adaptation strategies, Figure 9 shows the time history of the error velocity when either the control signal is updated every sample time (solid line) or every period (dashed line) of the oscillation. In Figure 9 the damping ratio of the system is either (a) $\zeta = 0.1$ or (b) $\zeta = 0.5$, the sampling frequency is set to forty samples per period and the convergence coefficient α is set to the optimal value that minimise the convergence time. The graph shows that the two adaptation strategies have very similar convergence for low values of damping ratio (plot (a)). However when the damping in the system under control is higher (plot (b)) a better performance can be obtained updating the control signal every sample. Although the difference in the convergence time between the two algorithms is only about two periods of the oscillation as shown in Figure 8 (b), the sample by sample adaptation offers a smoother convergence. This is because the time constant of the system gets shorter for higher values of damping ratio thus the adaptation can be carried out more rapidly. A rapid period by period adaptation means abruptly variation of the control signal which may degrade the performance of the control algorithm.

4. Conclusions

This paper is concerned with the vibration control of a single degree of freedom system excited by a harmonic force. A feedforward control algorithm in which the coefficients of the controller are updated either every sample time or every period of the oscillation has been considered. An equivalent feedback formulation for the two adaptation strategies has been derived. When the adaptation is carried out every sample time an equivalent time invariant feedback formulation at the sample rate can be obtained. However when the adaptation of the control coefficient is updated every period an equivalent feedback can only be obtained if the system is treated as being multi-rate. Simulation results have shown that if the error signal is sampled at sufficiently high rate the sample by sample adaptation strategy convergences faster than the period by period adaptation strategy for this single

degree of freedom plant. If the error signal is sampled only for few times every period then the period by period adaptation outperforms the sample by sample one. It has been also shown that the same conclusions can be drawn regardless the damping ratio in the system.

Acknowledgment
The work carried out by Michele Zilletti was supported by the EPSRC through the 'Engineering Nonlinearity' program (grant number EP/K003836/1).

References
[1] P. Lueg, Process of silencing sound oscillations., in, 1936.
[2] W.B. Conover, Fighting Noise with Noise, Noise Control, 2 (1956) 78-92.
[3] B. Widrow, S.D. Stearns, Adaptive signal processing, Prentice-Hall, Inc., Englewood Cliffs, NJ, 1985.
[4] S.J. Elliott, Signal Processing for Active Control, in, Academic Press, London, 2001.
[5] S.M. Kuo, D.R. Morgan, Active noise control systems: algorithms and DSP implementations, John Wiley & Sons, Inc., 1995.
[6] S.J. Elliott, I. Stothers, P.A. Nelson, A multiple error LMS algorithm and its application to the active control of sound and vibration, Acoustics, Speech and Signal Processing, IEEE Transactions on, 35 (1987) 1423-1434.
[7] S. Daley, I. Zazas, A recursive least squares based control algorithm for the suppression of tonal disturbances, Journal of Sound and Vibration, 331 (2012) 1270-1290.
[8] M.W. Davis, Refinement and evaluation of helicopter real-time self-adaptive active vibration controller algorithms, in, NASA Contractor report 3821, 1984.
[9] A.S. Jacklin, Comparison of five system identification algorithms for rotorcraft higher harmonic control, in, NASA Report TP-1998-207687, 1998.
[10] W. Johnson, Self-Tuning regulators for multicyclic control, in, NASA Technical paper 1996, 1982.
[11] D. Patt, L. Liu, J. Chandrasekar, D.S. Bernstein, P.P. Friedmann, Higher-Harmonic-Control Algorithm for Helicopter Vibration Reduction Revisited, Journal of Guidance, Control, and Dynamics, 28 (2005) 918-930.
[12] M. Zilletti, S.J. Elliott, M. Ghandchi Tehrani, Adaptive control of tonal disturbance in mechanical systems with nonlinear damping, Journal of Vibration and Control, (2015).
[13] G.P. Eatwell, Tonal noise control using harmonic filters, in: ACTIVE 96, Newport Beach, CA, USA, 1995, pp. 1087-1096.
[14] M. Bodson, S.C. Douglas, Adaptive algorithms for the rejection of sinusoidal disturbances with unknown frequency, Automatica, 33 (1997) 2213-2221.
[15] J. Tornero, G. Yuping, M. Tomizuka, Analysis of multi-rate discrete equivalent of continuous controller, in: American Control Conference, 1999. Proceedings of the 1999, 1999, pp. 2759-2763 vol.2754.